On the Bonding Characteristics of Clays and Biopolymers for Sustainable Earthen Construction

Rebecca A. Mikofsky(✉), Samuel J. Armistead, and Wil V. Srubar III

University of Colorado at Boulder, Boulder, CO 80309, USA
remi8173@colorado.edu

Abstract. Sustainable earthen building materials provide a pathway to mitigating the environmental impacts of the modern construction sector. While the application of these materials has been limited due to the inherent heterogeneity, erosivity, and weak mechanical properties of soil, the physical and thermal properties can be improved through the addition of ubiquitous, non-toxic, sustainable biopolymers. Yet, the fundamental understanding of the physiochemical bonding mechanisms between clays and biopolymers in this system is limited. In this work, a 'micro to macro' methodological approach was applied to investigate the bonding characteristics of common clays and clay-stabilizing biopolymers. At the micro-scale, fundamental interactions of clays (*i.e.,* kaolinite, bentonite) with biopolymer additives (*i.e.,* xanthan gum, guar gum, sodium alginate, microcrystalline cellulose) were assessed through mineral binding characterization techniques, including Fourier-transform infrared spectroscopy (FTIR) and thermogravimetric analysis (TGA). The findings were used to interpret unconfined compressive strength (UCS) tests results for macro-scale soil-biopolymer composites samples (1% biopolymer by soil mass). The results from this study illustrate the utility of understanding the mechanisms of clay-biopolymer interactions for improving the design of strong and durable earthen materials and structures.

Keywords: Earthen materials · Soil stabilization · Biopolymer · Clay · Binding affinity

1 Background

Earthen materials present an opportunity to reduce the high environmental impact of building construction by replacing conventional structural building materials such as concrete. Earthen materials and assemblies (*e.g.,* cob, rammed earth, adobe) are locally sourced and require minimal processing, therefore mitigating the high temperatures and transportation energy costs typically associated with traditional building materials. In addition to their low environmental impacts, these materials have been shown to have valuable material properties (*e.g.,* thermal, hygroscopic) and practical characteristics (*e.g.,* low cost, global availability). Despite these promising qualities, earthen materials often exhibit heterogeneity, erosivity, and weak mechanical properties, preventing their widespread use [1, 2].

S. Amziane et al. (Eds.): ICBBM 2023, RILEM Bookseries 45, pp. 280–292, 2023.
https://doi.org/10.1007/978-3-031-33465-8_22

Current research in geotechnical, civil engineering, and architectural design has shown that biopolymer additives can be used to improve the physical and chemical properties of soil and earthen materials. Biopolymer additives are non-toxic, low cost, and derived from naturally occurring sources. While many biopolymers have been investigated *via* trial and error ('top down' exploration), there is a fundamental lack of understanding of the molecular interactions responsible for the binding (or lack thereof) between soils and biopolymers. This study investigates these molecular interactions through a 'micro to macro' approach, in order to establish selection criteria for optimal soil-biopolymer composites.

Earthen materials are typically composed of subsoil containing a majority of sand 'aggregates' (50% or less) with a minority of cohesive clay 'binders'. According to the literature, soil for earth construction should include 15–30% clay content [3]. Clay minerals are classified as aluminum phyllosilicates with layers of octahedral alumina oxide and tetrahedral silica oxide sheets. The main categories of clays are illite, smectite, and kaolinite clays based on the arrangement of these sheets (2 tetrahedral : 1 octahedral, 2:1 and 1:1, respectively). Within the smectite category, bentonite (also known as montmorillonite) is the most commonly found variety and is highly expansive due to its 2:1 structure, which allows water to bind the groups of Si-Al-Si layers. Within the kaolin category, kaolinite is the most commonly available kaolin clay mineral and has a more tightly bound 1:1 structure. Bentonite and kaolinite were chosen in this work to serve as model clay systems. Clay (15% by weight) and sand (85% by weight) mixtures were designed to function as model earthen material systems for structural material property testing.

Table 1. Biopolymer Properties.

Biopolymer	Source	Stability	Water Solubility	Charge
Cellulose	plants	excellent thermal	mostly insoluble	non-ionic
Guar Gum	seeds	excellent	cold	non-ionic
Sodium Alginate	algae	limited	cold	anionic
Xanthan Gum	microbes	excellent	cold	very anionic

Biopolymers represent a broad category of biologically derived organic materials. Biopolymers are extracted from a variety of sources (*e.g.,* plant, bacteria, algae, fungi) and exhibit a wide range of chemical and physical properties. Polysaccharides, for example, are highly abundant in nature and are currently employed in large-scale commercial use (*e.g.,* food, packing, tissue engineering). They contain a plethora of chemically distinct monosaccharide monomer units linked through glycosidic bonds to create linear, branched, and network biopolymers. Four polysaccharides (*i.e.,* cellulose, sodium alginate, guar gum, and xanthan gum) were selected for this study based on their differing properties summarized in Table 1. Cellulose (C) is a linear polymer of β-(1 → 4)-linked D-glucose. The linear structure of cellulose causes it to become crystalline and insoluble in water. Guar gum (GG) has a β-(1 → 4)-linked D-mannose backbone with an

α-(1 → 6)-linked D-galactose side chain on alternating mannose units [4–6]. Guar gum is nonionic and stable across a large pH range [4–6]. Sodium alginate (SA) is a sodium salt of alginic acid, which is (1 → 4)-linked β-D-mannuronic acid and α-L-guluronic acid [7]. Sodium alginate is anionic and sensitive to pH, affecting viscosity and solubility [7]. Xanthan gum has a backbone of β-(1 → 4)-linked D-glucose backbone with trisaccharide (glucuronic acid, mannose, mannose) side-chains on alternating glucose units [8]. Xanthan gum is negatively charged and highly soluble due to its branched structure and side chain units [8]. These biopolymers represent a range of properties including different charges, different sources, different impacts due to change in pH, and different monosaccharide subunits.

The aim of this study was to explore the molecular interactions between two clay minerals, bentonite and kaolinite, and four biopolymers, namely cellulose, guar gum, sodium alginate, and xanthan gum. Doing so uncovered the chemical interactions of these biopolymers (or lack thereof) with common clay minerals. Mineral binding characterization methods developed in Armistead *et al.* (2020) were employed using thermogravimetric analysis (TGA) and attenuated total reflection Fourier-transform infrared (ATR-FTIR) spectroscopy [9]. Following micro-scale investigations, the mechanical properties of biopolymer-stabilized model earth systems were characterized using unconfined compressive strength (UCS) testing. By performing a 'micro to macro' approach, this study aimed to identify which of these biopolymers bind to specific clay minerals and which would be effective as property-improving additives for earthen materials.

2 Materials and Methods

2.1 Materials

Ultra-pure water was obtained from a Milli-Q purification system. Kaolinite (K) and bentonite (B) clay minerals were obtained from Sigma Aldrich. Ottawa sand (80% passing 30–40 mesh, resulting in a 0.42–0.6 mm particle size) was obtained from VWR Chemicals BDH. Guar gum from *Cyamopsis tetragonoloba* seeds, xanthan gum from *Xanthomonas campestris* bacteria, sodium alginate salt from brown algae, and microcrystalline cellulose were purchased from Sigma Aldrich. Molar mass was determined using average molar mass for the polymeric sub-units giving 162.14, 180.16, 176.12, 204.56 g/mol for cellulose (C), guar gum (GG), sodium alginate (SA), and xanthan gum (XG) [9, 10]. Commercial 37% Hydrogen Chloride and LabChem 25% Ammonium Hydroxide were used for pH adjustments.

2.2 Clay Characterization

Clays were dried in a furnace at 110 ± 10 °C for 5 h, pestled in small batches for 1 min, then sieved to obtain particles < 45 microns using a Gilson SS-3 sieve shaker. The median particle size (d50) was measured to be 4.75 μm for B and 8.66 μm for K using a Malvern Panalytical Mastersizer 3000 with a HydroMV dispersion accessory (Fig. 1). Stirring (2500 rpm) and sonication (50% power) were used to disperse clay in water and achieve a laser obscuration (5–15%) based on the particle size range.

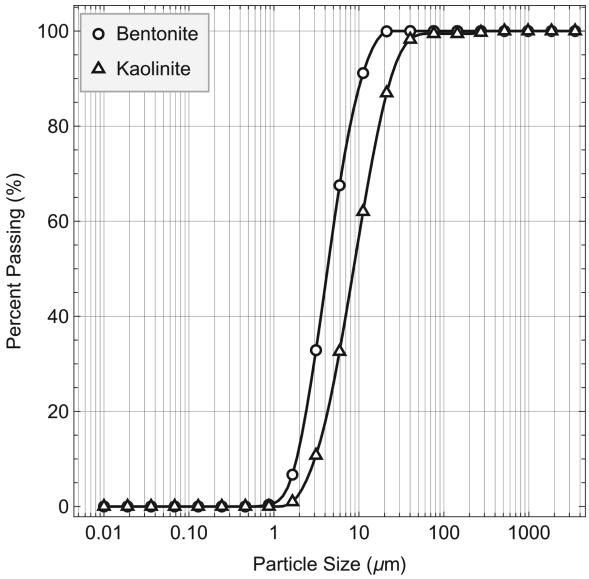

Fig. 1. Particle size distribution for bentonite and kaolinite.

Clay compositions were confirmed using X-ray diffraction spectroscopy (Bruker D8 single-crystal X-ray diffractometer) with a step size of 0.019, 2 s/step, and a 0.02 mm divergence slit. Clay samples for XRD were prepared by suspending clay in water and drying in air on a quartz slide. Diffractograms showed that the bentonite clay sample included montmorillonite, quartz, and plagioclase feldspar (Fig. 2a), and the kaolinite clay sample included kaolinite and quartz (Fig. 2b) [11–13]. ATR-FTIR confirmed these results [14, 15].

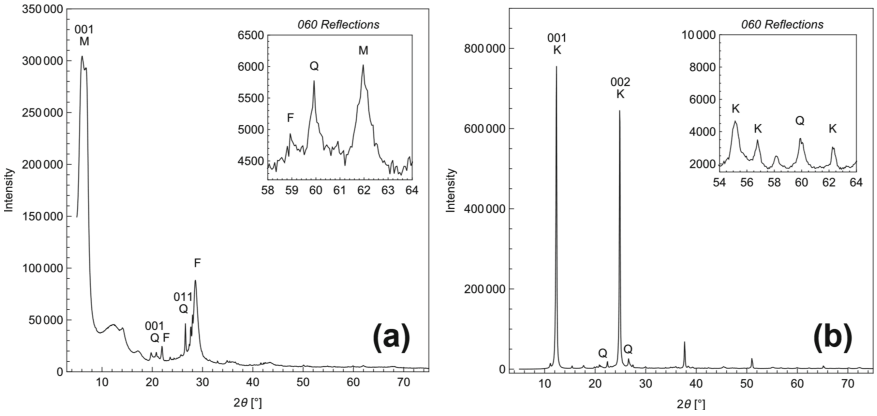

Fig. 2. XRD analysis for (a) bentonite and (b) kaolinite. M = montmorillonite, Q = quartz, F = feldspar, K = kaolinite.

2.3 Mineral Binding Characterization

Mineral binding characterization (MBC) was performed in accordance with Armistead *et al.* [9]. Compositions for each mineral binding characterization sample is listed in Table 2. Biopolymer solutions (0.01 M) were first prepared by slowly adding biopolymer powder to heated (40 °C) ultra-pure water whilst under simultaneous agitation (stir bar, 600 rpm). Then, the solution was held at 40 °C for 10 min with continuous stirring. The solution (20 mL) was poured into centrifuge tubes (50 mL) and ultrasonicated (Branson 2510) for 10 min. Solutions were used within 24 h of preparation and stored away from light. Clay (50 mg) was added to described biopolymers solutions, followed by ultrasonication for 10 min. Then, pH was adjusted to ±1.0 of the desired pH value

Table 2. Sample Composition for MBC Testing

Sample	Clay	Biopolymer	pH
B-C-5	Bentonite (50 mg)	Cellulose (20 mL 0.01M)	5
B-C-7			7
B-C-9			9
B-GG-5		Guar Gum (20 mL 0.01M)	5
B-GG-7			7
B-GG-9			9
B-SA-5		Sodium Alginate (20 mL 0.01M)	5
B-SA-7			7
B-SA-9			9
B-XG-5		Xanthan Gum (20 mL 0.01M)	5
B-XG-7			7
B-XG-9			9
K-C-5	Kaolinite (50 mg)	Cellulose (20 mL 0.01M)	5
K-C-7			7
K-C-9			9
K-GG-5		Guar Gum (20 mL 0.01M)	5
K-GG-7			7
K-GG-9			9
K-SA-5		Sodium Alginate (20 mL 0.01M)	5
K-SA-7			7
K-SA-9			9
K-XG-5		Xanthan Gum (20 mL 0.01M)	5
K-XG-7			7
K-XG-9			9

(*i.e.,* 5, 7 or 9) using a few drops of 0.5 M HCl or 0.1 M NH_4OH. These pHs were chosen to investigate sample stability or changes in binding affinity, through a range of pH values. Samples were mixed with a Labnet Mini LabRoller Rotator for 30 min. Samples were washed four times to remove unbound biopolymer. For the washing procedure, the sample was first centrifuged at 4000 rpm for 10 min. Then, the supernatant was removed, and 20 mL of ultra-pure water was added. The process was repeated four times for a total of five centrifuge cycles. After final centrifuging and supernatant removal, samples were left to dry in air at room temperature. After drying, samples were characterized using TGA and ATR-FTIR.

TGA (TA Discovery TGA 5500) was performed in N_2 gas from 50 to 800 °C with a ramp rate of 5 °C/min. Percent mass loss was calculated from 200 to 400 °C in the range in which the combustion of organic materials is most likely to occur. ATR-FTIR (Thermo Scientific Nicolet iS20 with a Ge Crystal ATR accessory) was performed using 64 scans, 4 cm^{-1} resolution. For comparison, pure clay was measured using TGA and FTIR, and air-dried biopolymer samples (0.1 M) were measure using FTIR.

2.4 Compressive Strength Testing

Cubic samples were created for compressive strength testing (Table 3). Model earthen materials were created by mixing clay (15 wt_{soil} %) with Ottawa sand (85 wt_{soil} %). First, dry biopolymer powder (1 wt_{soil} %) was mixed with the clay-sand mixture. Then, ultra-pure water was added achieve a moldable workability for the K-(22.5 wt_{soil} %) and B-containing mixtures (45 wt_{soil} %) and thoroughly mixed. Each clay-sand-biopolymer mixture was placed into 1.25 in (31.75 mm) cubic silicone molds. All samples were prepared at the same time and left to cure in an ambient environment. The surface was

Table 3. Sample Composition for Mechanical Testing

Sample	Clay (wt_{clay} /wt_{soil})	Sand (wt_{sand} /wt_{soil})	Biopolymer (wt_{bp} /wt_{soil})	Water (wt_{water} /wt_{soil})
B-NONE	15% Bentonite	85% Ottawa sand	-	22.5% water
B-C			1% Cellulose	
B-GG			1% Guar Gum	
B-SA			1% Sodium Alginate	
B-XG			1% Xanthan Gum	
K-NONE	15% Kaolinite	85% Ottawa sand	-	45% water
K-C			1% Cellulose	
K-GG			1% Guar Gum	
K-SA			1% Sodium Alginate	
K-XG			1% Xanthan Gum	

smoothed using a spatula, and the samples were left to dry in air until firm enough to be pressed out of the mold (at least 24 h). Mechanical testing on triplicate samples was performed 96 h after casting, when the samples achieved constant mass (fully dried). Unconfined compressive strength was measured using an Instron Universal Testing machine with a 5 kN load cell and 1.5 mm/min displacement-controlled rate. Maximum compressive strength was obtained for each sample.

3 Results and Discussion

3.1 Mineral Binding Characterization

TGA results, shown in Fig. 3, illustrate that all samples exhibited a characteristic loss in mass with increasing temperature. Mass loss between 200–400 °C indicates the presence of biopolymer and higher biopolymer-clay affinity. For both bentonite (B) and kaolinite (K), the addition of cellulose resulted in the highest mass loss, with B-C pH 7 having the highest mass loss overall for bentonite (26.98%) and K-C pH 9 having the greatest mass loss for kaolinite (13.79%). Guar gum resulted in the second highest mass loss for both bentonite (11.67% for pH 5) and kaolinite (9.58% for pH 5). Values for sodium alginate and xanthan gum (< 1.1%) suggest that negligible quantities of those biopolymers bound to the clays.

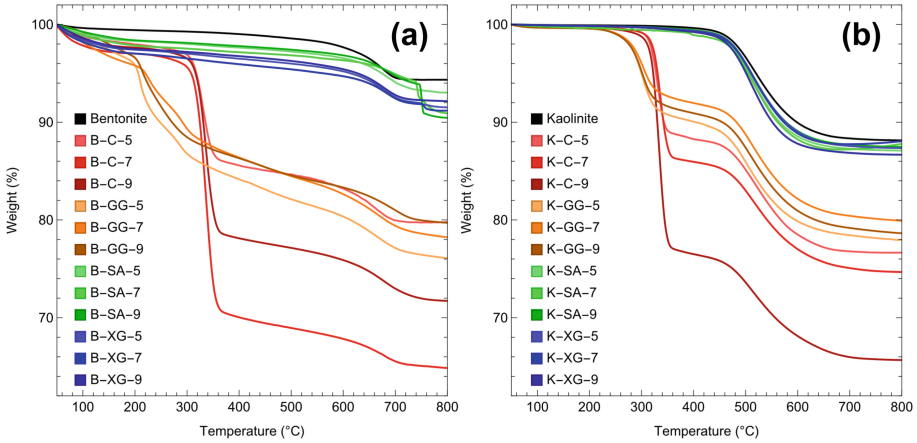

Fig. 3. TGA results for (a) bentonite- and (b) kaolinite-biopolymer mixtures. B = bentonite, K = kaolinite, C = cellulose, GG = guar gum, SA = sodium alginate, XG = xanthan gum.

All FTIR spectra are shown in Fig. 4. The comparison of FTIR spectra of pure clay, clay-biopolymer, and pure biopolymer samples could indicate the presence of biopolymer bound to the clay after washing. When analyzing bentonite and kaolinite control samples, a set of peaks was observed between 600–1200 cm^{-1}, attributable primarily to the Si-O stretching in kaolinite and bentonite [14, 15]. Within this region, peaks due to the octahedral oxide sheets (*e.g.,* AlMg-OH, AlFe-OH, AlAl-OH) or OH of inner hydroxyl groups in kaolinite can occur depending on the specific clay sample [14, 15]. Therefore changes to the 1200–1800 cm^{-1} and 2800–3800 cm^{-1} regions were investigated for evidence of biopolymer binding. These regions contain peaks characteristic of polysaccharides: C-H bending (1330–1470 cm^{-1}), COO- asymmetric stretching (weak at 1400 cm^{-1}, strong at 1600 cm^{-1}), and O-H stretching (3000–3500 cm^{-1}) [16, 17].

FTIR results for the bentonite-guar gum samples (Fig. 4b) indicate biopolymer presence within the 1200–1800 cm^{-1} and 2800–3800 cm^{-1} regions. However, these changes from the pure bentonite FTIR spectra can be seen in all bentonite-biopolymer samples. Notably, a sharp peak can be observed at 1630 cm^{-1} and a broad peak at 3300 cm^{-1}, which are associated with moisture in the bentonite structure [18]. This result is an indication that physiosorbed water, and perhaps biopolymer, is still present within the samples. This concept will be explored in further studies.

The FTIR results corroborate the TGA results that also indicated the presence of bound guar gum in the bentonite and kaolinite samples. While the TGA results suggested that more cellulose was bound to the clays than guar gum, the FTIR results in Fig. 4a suggest that cellulose does not chemically bind to kaolinite. These findings suggest (a) that the cellulose may physisorb onto clay surfaces through van der Waal's forces rather than chemically bond and/or (b) the cellulose was not removed during the washing cycles due to its insolubility in water.

For kaolinite samples (Fig. 4e-h), in line with TGA results, the introduction of new peaks can be observed within guar gum spectra, an indication of chemisorption between the two components. This result is consistent with the TGA results, which also indicated high biopolymer affinity. In contrast, considering sodium alginate, xanthan gum and cellulose additives imparted little change in the FTIR spectra throughout the pH range indicating little bonding to kaolinite.

One key factor to inform whether physisorption or chemisorption is occurring is to interpret these results through surface charge. Bentonite has an isoelectric point of 2.5 pH, meaning it will be negatively charged across the pH range investigated (5–9) [19, 20]. Similarly, kaolinite has a negative zeta potential in the range, but a higher isoelectric point of 3.5–4.6 pH [19, 21]. As noted in Table 1, guar gum is the only biopolymer that is neutral, highly soluble and branched. These properties, as shown in the results, allow it to bind more readily with the negatively charged surface of the clays than the negatively charged sodium alginate or xanthan gum. While cellulose is similarly nonionic, it does not bind due to its linear, insoluble nature, preventing binding interactions with the clay surface.

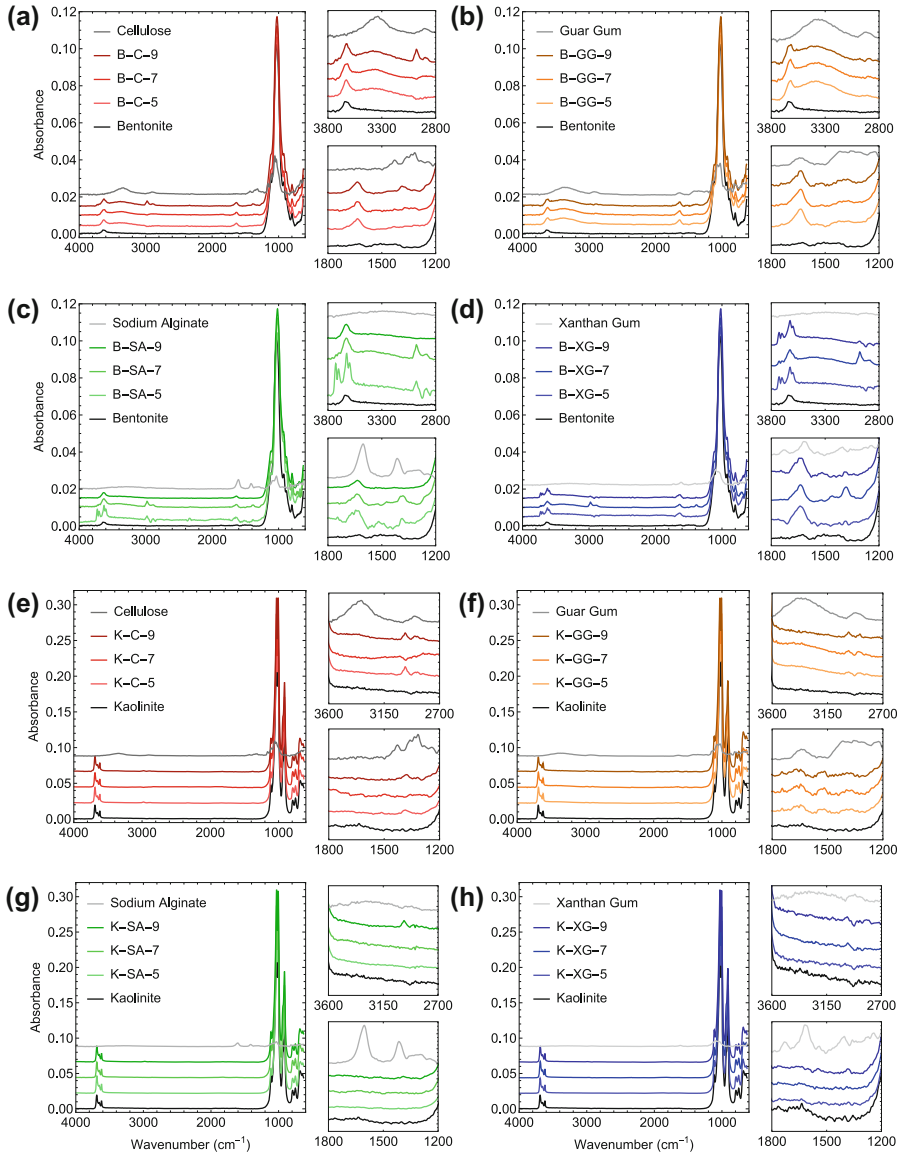

Fig. 4. ATR-FTIR of (a-d) bentonite and (e-h) kaolinite-biopolymer samples. B = bentonite, K = kaolinite, C = cellulose, GG = guar gum, SA = sodium alginate, XG = xanthan gum.

3.2 Compressive Strength Testing

Unconfined compressive strength testing was performed on sand-clay-biopolymer samples 96 hr after casting. Figure 5 shows stress strain curves (with slack removed) for

all clay-sand-biopolymer samples. The curves indicate that the choice of biopolymer influences both stress and strain properties.

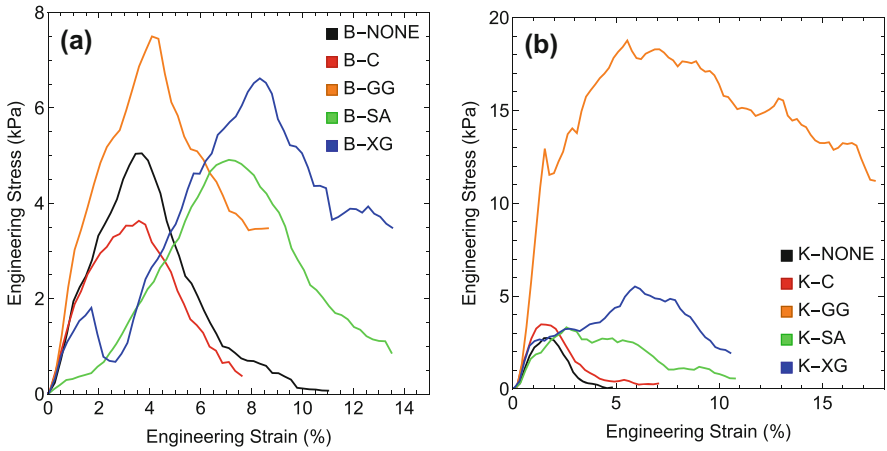

Fig. 5. Representative engineering stress-strain curves for Bentonite (a) and Kaolinite (b) samples with slack removed from loading curve.

Figure 6 shows maximum compressive strength. These results indicate that cellulose (C) and sodium alginate (SA) do not show a significant improvement in strength. Data suggests that these biopolymers neither bind to clays or sand nor do they undergo sufficient cross-linking to impart additional property changes to the soil. The addition of guar gum, in contrast, showed a 512% improvement for kaolinite-sand samples and 136% for bentonite-sand samples. These results are consistent with increased binding affinity to bentonite and kaolinite as measured *via* TGA for both bentonite and kaolinite and FTIR for kaolinite. Xanthan gum exhibited a 182% improvement for K-containing samples and the greatest increase in strength for bentonite-containing samples (152%).

It is hypothesized that xanthan gum has the greatest strength increase for bentonite-sand samples due to its high viscosity at low concentrations. The FTIR results indicate that there is some binding with clay, so while the binding affinity is lower than guar gum, it could have a greater than or similar due to the increased viscosity and the pseudoplastic properties of xanthan gum. For kaolinite-sand samples, xanthan gum resulted in a similar increase showing that it is not forming significant interactions with either kaolinite or bentonite but rather it is the basic properties of xanthan gum as a binder. Further experiments need to be performed to differentiate these effects and investigate the impacts of water and time on strength.

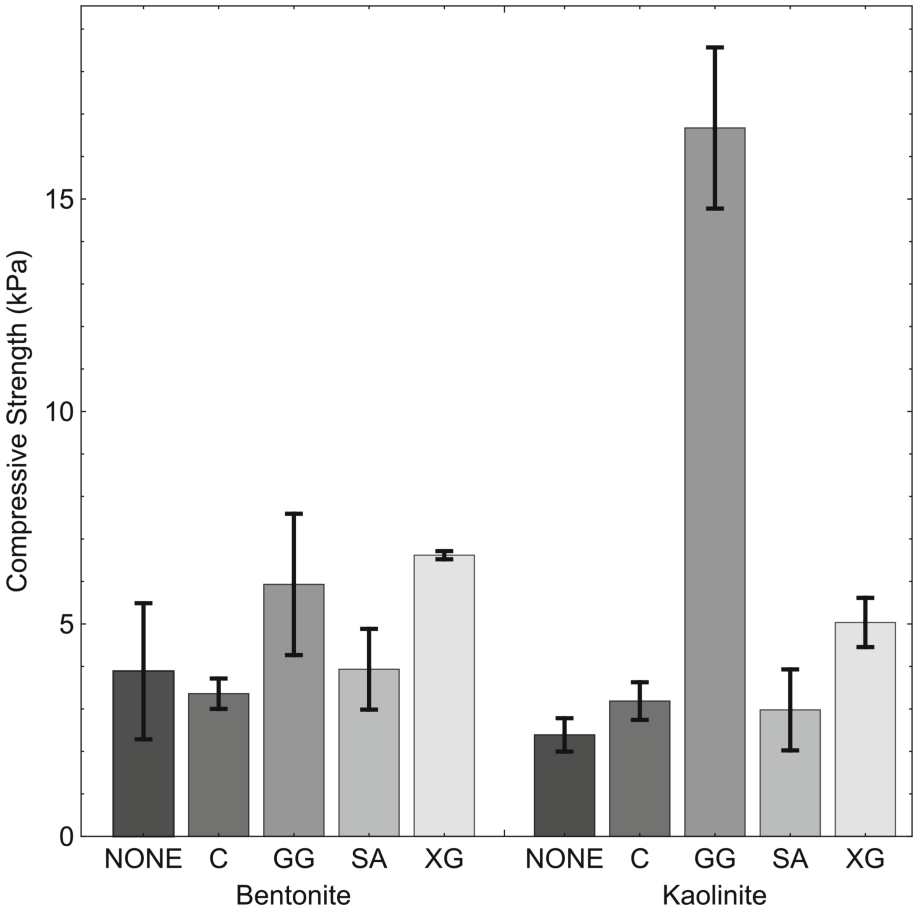

Fig. 6. Maximum compressive strength values sample for each clay. B = bentonite, K = kaolinite, NONE = no biopolymer, C = cellulose, GG = guar gum, SA = sodium alginate, XG = xanthan gum.

4 Conclusion

This paper presents an ongoing study on clay-biopolymer binding characteristics with the aim to enhance the physical properties of soils for construction. Earthen materials, a critical sustainable alternative for conventional materials such as concrete, exhibit superior environmental features but are not fully integrated in construction due to their inherent variability and weak mechanical properties. Using a 'micro to macro' approach, this research investigates the bonding characteristics of bentonite and kaolinite using four biopolymer additives: xanthan gum, guar gum, sodium alginate, and microcrystalline cellulose. The characterization includes Fourier-transform infrared spectroscopy (FTIR), thermogravimetric analysis (TGA), and unconfined compressive strength testing (UCS). The results show that kaolin-guar gum outperforms other clay-biopolymer mix designs in terms of its mineral binding characterization analysis and mechanical testing. This

finding is in line with theoretical knowledge based on surface charge of guar gum and kaolinite.

These preliminary results need to be verified using additional testing. Further experiments would include investigating the effect of different pH values and biopolymers, and testing the synergy of more than one biopolymer in combination with others. Methodological changes would include increasing FTIR signal for control biopolymers to improve comparability and integrating steps into the preparation procedure to ensure any physisorbed or insoluble biopolymer is removed.

Acknowledgements. This research was made possible by the Department of Civil, Environmental, and Architectural Engineering, the Materials Science and Engineering Program, the College of Engineering and Applied Sciences, and the Living Materials Lab at the University of Colorado Boulder. The editorial comments and suggestions received from Dr. Lola Ben-Alon at Columbia University are gratefully acknowledged. This work was supported by the National Science Foundation (Grant No. CMMI-2134488). Any opinions, findings, and conclusions or recommendations expressed in this material are those of the authors and do not necessarily reflect the views of the National Science Foundation.

References

1. Ben-Alon, L., Loftness, V., Harries, K.A., DiPietro, G., Hameen, E.C.: Cradle to site Life Cycle Assessment (LCA) of natural vs conventional building materials: a case study on cob earthen material. Build. Environ. **160**, 106150 (2019). https://doi.org/10.1016/j.buildenv.2019.05.028
2. Ben-Alon, L., Loftness, V., Harries, K.A., Hameen, E.C., Bridges, M.: Integrating earthen building materials and methods into mainstream construction. J. Green Build. **15**, 87–106 (2020). https://doi.org/10.3992/1943-4618.15.1.87
3. Jiménez Delgado, M.C., Guerrero, I.C.: The selection of soils for unstabilised earth building: a normative review. Constr. Build. Mater. **21**, 237–251 (2007). https://doi.org/10.1016/J.CONBUILDMAT.2005.08.006
4. Mudgil, D., Barak, S., Khatkar, B.S.: Guar gum: processing, properties and food applications—a review. J. Food Sci. Technol. **51**(3), 409–418 (2011). https://doi.org/10.1007/s13197-011-0522-x
5. Thombare, N., Jha, U., Mishra, S., Siddiqui, M.Z.: Guar gum as a promising starting material for diverse applications: a review. Int. J. Biol. Macromol. **88**, 361–372 (2016). https://doi.org/10.1016/j.ijbiomac.2016.04.001
6. Sharma, G., et al.: Guar gum and its composites as potential materials for diverse applications: a review. Carbohyd. Polym. **199**, 534–545 (2018). https://doi.org/10.1016/j.carbpol.2018.07.053
7. Nordgård, C.T., Draget, K.I.: Chapter 26 - Alginates. In: Phillips, G.O., Williams, P.A. (eds.) Handbook of Hydrocolloids, 3rd edn. pp. 805–829. Woodhead Publishing (2021). https://doi.org/10.1016/B978-0-12-820104-6.00007-3
8. Sworn, G.: Chapter 27 - Xanthan gum. In: Phillips, G.O., Williams, P.A. (eds.) Handbook of Hydrocolloids, 3rd edn. pp. 833–853. Woodhead Publishing (2021). https://doi.org/10.1016/B978-0-12-820104-6.00004-8
9. Armistead, S.J., Rawlings, A.E., Smith, C.C., Staniland, S.S.: Biopolymer stabilization/solidification of soils: a rapid, micro-macro. Cross-Discip. Appr. Environ. Sci. Technol. **54**, 13963–13972 (2020). https://doi.org/10.1021/acs.est.0c02001

10. Armistead, S.J., Smith, C.C., Staniland, S.S.: Sustainable biopolymer soil stabilization in saline rich, arid conditions: a 'micro to macro' approach. Sci. Rep. **12**, 2880 (2022). https://doi.org/10.1038/s41598-022-06374-6
11. Brindley, G.W., Brown, G.: Crystal Structures of Clay Minerals and their X-Ray Identification. Mineralogical Society (1982)
12. Moore, D.M., Reynolds, R.C., Reynolds, R.C.: X-ray Diffraction and the Identification and Analysis of Clay Minerals. Oxford University Press (1989)
13. Chipera, S.J.: Baseline studies of the clay minerals society source clays: powder X-ray diffraction analyses. Clays Clay Miner. **49**, 398–409 (2001). https://doi.org/10.1346/CCMN.2001.0490507
14. Madejová, J.: Baseline studies of the clay minerals society source clays: infrared methods. Clays Clay Miner. **49**, 410–432 (2001). https://doi.org/10.1346/CCMN.2001.0490508
15. Russell, J.D., Fraser, A.R.: Infrared methods. In: Wilson, M.J. (ed.) Clay Mineralogy: Spectroscopic and Chemical Determinative Methods, pp. 11–67. Springer, Dordrecht (1994). https://doi.org/10.1007/978-94-011-0727-3_2
16. Popescu, C.-M., Popescu, M.-C., Singurel, G., Vasile, C., Argyropoulos, D.S., Willfor, S.: Spectral characterization of eucalyptus wood. Appl. Spectrosc. **61**, 1168–1177 (2007). https://doi.org/10.1366/000370207782597076
17. Guo, Q., Ai, L., Cui, S.W.: Fourier Transform Infrared Spectroscopy (FTIR) for carbohydrate analysis. In: Methodology for Structural Analysis of Polysaccharides. SpringerBriefs in Molecular Science. Springer, Cham (2018). https://doi.org/10.1007/978-3-319-96370-9_9
18. Nazdracheva, T., Morozov, A., Yavna, V., Kochur, A.: Data on FTIR spectra of the clays KGa-1b and STx-1b and their mixtures at different moistures. Data Brief. **42**, 108282 (2022). https://doi.org/10.1016/j.dib.2022.108282
19. Schroeder, P.A. (ed.): Critical zone clay geochemistry. In: Clays in the Critical Zone. pp. 133–179. Cambridge University Press, Cambridge (2018)
20. Mekhamer, W.K.: Stability changes of Saudi bentonite suspension due to mechanical grinding. J. Saudi Chem. Soc. **15**, 361–366 (2011). https://doi.org/10.1016/j.jscs.2011.03.014
21. Yukselen, Y., Kaya, A.: Zeta potential of kaolinite in the presence of Alkali, Alkaline earth and Hydrolyzable metal ions. Water Air Soil Pollut. **145**, 155–168 (2003). https://doi.org/10.1023/A:1023684213383